Redox Chemistry of Gaseous Reactants Inside Photoexcited $FeAlPO_4$ Molecular Sieve

N. Ulagappan and H. Frei*

Physical Biosciences Division, Mailstop Calvin Laboratory, Lawrence Berkeley National Laboratory, University of California, Berkeley, California 94720

Received: August 24, 1999; In Final Form: November 21, 1999

The reactivity of ligand-to-metal charge transfer excited Fe centers of $FeAlPO_4$-5 molecular sieve at the gas−micropore interface has been probed by in situ FT-IR spectroscopy. Laser light in the region 350−430 nm was used to excite the metal centers, and reaction was induced between methanol or 2-propanol and O_2. Acetone and H_2O are the observed products of the 2-propanol + O_2 system, while the reaction of methanol with O_2 yields formic acid, methyl formate, and H_2O as final products. These originate from secondary thermal reaction of initially produced formaldehyde and hydrogen peroxide. The primary step of the proposed mechanism involves one-electron reduction of O_2 by transient Fe^{+II} under concurrent donation of an electron to the hole of framework oxygen by the alcohol molecule. The efficient reaction suggests that the photoreduced Fe center of the molecular sieve has a substantially stronger reducing power than the conduction band electrons of dense-phase Fe_2O_3 semiconductor particles.

I. Introduction

Transition metals play an essential role as chromophores or redox centers in some of the most important photoinduced transformations in chemistry and biology.[1] The central role of these metals has its origin in the wide range of optical absorption properties, the tunability of redox properties by ligand substitution, and the accessibility of multiple oxidation states. We are interested in exploring framework transition metals of microporous materials as chromophores and redox sites for light-induced chemistry at the gas−micropore interface. This approach to photochemistry is motivated by our recent finding that photoreaction of gas mixtures adsorbed onto zeolites results in product selectivities that exceed by far those achieved for the same reactions in homogeneous solution or the gas phase.[2] Kinetic studies of prototype radical pairs by nano- and microsecond FT-infrared spectroscopy revealed an important mechanistic clue to the high selectivity, namely predominant reaction of geminate radical pairs, as indicated by single-exponential behavior of the radical decay.[3] Nongeminate, product-scrambling encounters of the radicals do not occur in the systems studied so far. At the same time, the lifetimes of the radicals were found to be unexpectedly long; they range from tens to hundreds of microseconds even at room temperature, exceeding those in homogeneous solution or the gas phase by orders of magnitude. These unique properties of photogenerated radical pairs inside microporous solids, a very long lifetime, and lack of scrambling reactions make photochemistry in solvent-free molecular sieves a promising approach to efficient and selective chemical transformations. Therefore, it is natural to explore the possibility of combining the use of transition metals and microporous environments by conducting light-induced gas-phase chemistry in molecular sieves that feature metal centers as part of the framework.

Several gas-phase photochemical reactions in Ti- or V-substituted microporous silicates have been reported by Anpo and co-workers. The authors demonstrated photocatalytic activity of the framework metal centers principally by luminescence quenching experiments and monitoring of reactivity by chromatographic analysis of the desorbed products.[4−10]

Essential for designing photochemical synthesis in such microporous solids is the knowledge of the redox properties of the excited metal centers. Redox potentials at the gas−solid interface might differ substantially from those in solution, yet no data are available in the case of transition metal molecular sieves. One way of determining the redox energetics at the gas−solid interface is to conduct photochemical probe reactions. In situ detection of primary products would furnish the mechanistic insight needed for establishing the primary photochemical step and, hence, allow us to gain information on the energetics of the excited-state initiating the reaction. In this paper, we report photochemical studies in order to probe the reactivity of the excited Fe−O ligand-to-metal charge-transfer (LMCT) state of the iron-substituted aluminophosphate sieve with AFI structure,[11] $FeAlPO_4$-5 (abbreviated FAPO-5), at the gas−micropore interface. Low alcohols (methanol, 2-propanol) are used as donors, O_2 as an electron acceptor. The chemistry is monitored in situ by FT-infrared spectroscopy. We chose an $AlPO_4$ sieve because isomorphous substitution of a greater variety of transition metals has been reported in the case of aluminophosphates than for silicates.[12] Among these, the large-pore FAPO-5 sieve is one of the best characterized materials.[13−19] It consists of a one-dimensional system of 7.3 Å diameter channels with a pore volume of 0.18 $cm^3\ g^{-1}$.[18,20]

II. Experimental Section

FAPO-5 molecular sieve was synthesized according to published procedure,[20] with minor modifications. A gel of composition $1Al_2O_3/1P_2O_5/1Et_3N/0.02Fe_2O_3/40H_2O$ was prepared using Catapal B alumina (Vista), *ortho*-phosphoric acid (85%, Fluka), triethylamine (Fluka), $Fe(NO_3)_3{\cdot}9H_2O$ (Fluka), and distilled water as source material. One-half of the amount of water was mixed with the alumina source, while phosphoric acid and iron nitrate were dissolved in the other half. The two aqueous systems were separately mixed, after which the

10.1021/jp992991c CCC: $19.00
Published on Web 12/30/1999

$Fe(NO_3)_3-H_3PO_4$ solution was added dropwise to the alumina−water slurry. The resulting mixture was stirred vigorously for 20 min in order to achieve a homogeneous mixture. The template, triethylamine, was added dropwise, and the gel was homogenized for 30 min. The initial pH was 3.5. About 80 mL of the gel were loaded into a 120 mL Teflon-lined autoclave and heated to 448 K in an air-circulated oven for 24 h. The gel transformed into a well-settled solid suspended in water (pH 7.4). The collected solid was washed repeatedly with water and separated by decanting. Final drying was done at 383 K.

Powder XRD of the material revealed high crystallinity and confirmed the AFI topology of the of the molecular sieve.[11,21] No other phase was detected. Calcination of FAPO-5 was conducted at 823 K overnight under flow of oxygen. XRD of the calcined material again did not show any additional phase. To rule out any extraframework Fe ions, the calcined sieve was exchanged with a 1% aqueous NaCl solution. The material appeared white, indicating the absence of extraframework iron oxide. Since, during the calcination process, extraframework iron sinters to Fe_2O_3 particles,[14] optical spectroscopy can be employed to detect nonframework iron. On adding 1 wt % iron oxide to $AlPO_4$-5 powder, UV−vis reflectance spectra showed intense peaks at 540 and 395 nm, which are characteristic of Fe_2O_3. Absorption due to Fe_2O_3 particles was completely absent in the spectrum of neat FAPO-5. Taking into account the detection limit (peak-to-peak noise in the 450−540 nm region) of the FAPO-5 spectrum and the observed Fe_2O_3 absorbance in the $Fe_2O_3/AlPO_4$-5 spectrum, an upper limit of 1% of all Fe in FAPO-5 was estimated to be extraframework. Such a low concentration of extraframework Fe is in agreement with more recent reports on the synthesis and characterization of this material.[18] The $AlPO_4$-5 sieve used in this study was prepared by the same procedure as FAPO-5 without the iron source. Refined unit cell parameters derived from XRD data of the resulting material were $a = b = 13.85 \pm 0.08$ Å, $c = 8.47 \pm 0.05$ Å.[22] The increase of the cell parameters relative to those of $AlPO_4$-5 is consistent with substitution of Fe into the framework.[21] ICP-AES analysis of calcined FAPO-5 revealed an Fe/(Al + P) ratio of 0.012. Infrared spectroscopy did not indicate any Bronsted acid sites, and Lewis acidity was found to be negligible.[23]

UV−vis spectra were recorded in the diffuse reflectance mode with a Shimadzu model UV-2100 spectrometer equipped with an integrating sphere model ISR-260. $BaSO_4$ powder or a pressed pellet of $AlPO_4$-5 were used as reference.

FT-IR instrumentation, vacuum equipment, and experimental procedures were similar to those previously described.[24] In short, self-supporting FAPO-5 wafers of 12 mm diameter and approximately 12 mg weight were prepared with a KBr press under 4 ton pressure for 3 min. The pellet was mounted in a miniature vacuum cell connected to a manifold for gas loading. The cell was equipped with CaF_2 windows and mounted inside an Oxford cryostat model Optistat. A temperature controller model ITC-502 allowed tuning of the pellet temperature from 77 to 473 K. For each experiment, a fresh pellet was prepared and dehydrated at 473 K under high vacuum overnight using a turbomolecular pump (Varian model V-60). In situ infrared monitoring was conducted with an IBM-Bruker IR-97 spectrometer at 1 cm^{-1} resolution. Pressed aluminophosphate pellets transmit infrared light in the region above 1300 cm^{-1}. Photochemistry was induced by irradiation of the pellet with the 355 nm output of a pulsed Nd:YAG laser Quanta Ray model DCR-2 (10 Hz) or the emission of a Nd:YAG pumped dye laser (PDL-1) at 389 nm (LD390) or 423 nm (Stilbene 420).

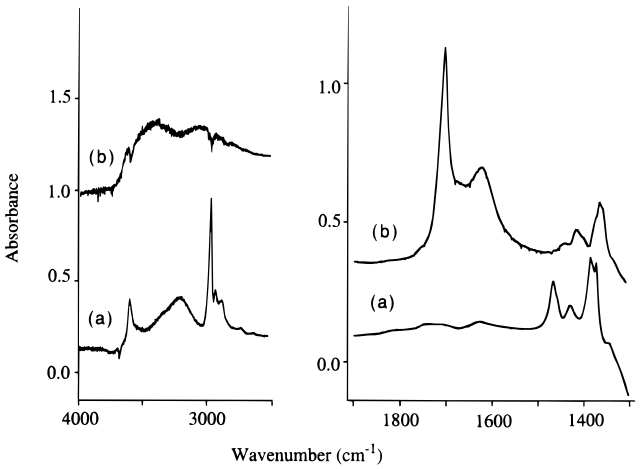

Figure 1. (a) Infrared difference spectrum of FAPO-5 pellet loaded with 2-propanol and 250 Torr O_2 gas at 21 °C. (b) Infrared difference spectrum after 355 nm irradiation at 145 mW cm^{-2} for 90 min.

2-Propanol (Aldrich, 99.9%), methanol (EM Science, 99.8%), methanol-d_4 (Aldrich, 99%), and acetone (EM Science, 99.5%) were degassed by vacuum distillation or freeze−pump−thaw cycles. Oxygen gas (Air Products, 99.997%) and $^{18}O_2$ gas (MSD Isotopes, 97.6% ^{18}O) were used as received. Paraformaldehyde (Aldrich, 95%) and perdeuteroparaformaldehyde (Cambridge Isotope Laboratories, 99% D) were depolymerized, and the product was purified according to the literature procedure.[25]

III. Results

We will first present oxidation of 2-propanol with O_2 under photoexcitation of the FAPO-5 framework, followed by our results on methanol photooxidation in this metal-substituted molecular sieve.

1. Photooxidation of 2-Propanol by O_2. When loading a few Torr of 2-propanol gas into a dehydrated FAPO-5 pellet at room temperature, a substantial pressure drop indicated instantaneous uptake into the channels of the sieve. Concentrations were typically one molecule per six unit cells, as determined by manometric measurements. At the same time, infrared monitoring revealed an intense spectrum with bands at 1345 (shoulder), 1374, 1388, 1432, 1468, 2734, 2904, 2936, 2997, 3200, and 3605 cm^{-1}, as shown in Figure 1, trace a. All absorptions are characteristic of 2-propanol. Frequencies are very close to those of free 2-propanol, indicating little perturbation by the solid. An exception is the very broad band at 3200 cm^{-1}, which originates from 2-propanol OH groups hydrogen-bonded to the channel wall. Framework P−OH groups interacting with adsorbed 2-propanol molecules may also contribute to this absorption since loading of the alcohol is accompanied by a depletion of the free P−OH band at 3674 cm^{-1} (Figure 1a). Addition of 250 Torr of O_2 gas did not result in any spectral changes, even when leaving the matrix overnight at room temperature.

Excitation of the FAPO-5 ligand-to-metal charge-transfer transition[18] with 355 nm light resulted in a decrease of the 2-propanol infrared bands. As can be seen from the diffuse reflectance spectrum of Figure 2, the charge-transfer absorption appears as a structureless tail extending from the UV into the blue spectral region. Concurrent product growth was observed at 1363, 1418, 1625(5), 1711(30), and 3400 cm^{-1} (very broad). Numbers in parentheses indicate ^{18}O isotope shifts of the peaks when conducting the photoreaction with $^{18}O_2$. The infrared difference spectrum following 355 nm irradiation for 90 min is

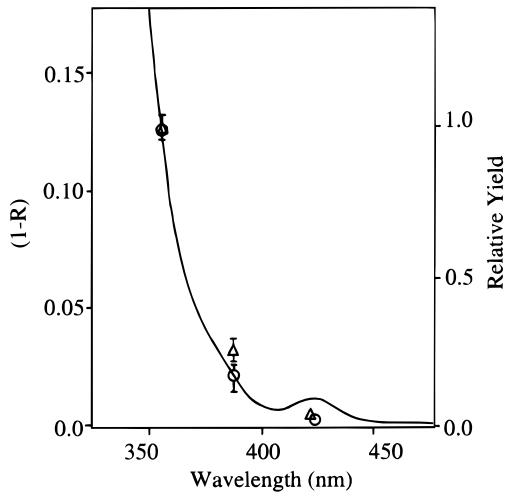

Figure 2. Diffuse reflectance spectrum of FAPO-5 molecular sieve (evacuated) at room temperature. Data points indicate relative product yields of 2-propanol + O_2 (△) and methanol + O_2 (○) photoreaction for fixed photolysis photon flux and duration at 355, 389, and 423 nm.

shown in Figure 1, trace b. Photoreaction was negligible when (metal-free) $AlPO_4$-5 sieve was used. Absorption frequency and ^{18}O shift of the most intense product peak at 1711 cm^{-1} indicate the growth of a carbonyl product, most probably acetone. The 1361 and 1418 cm^{-1} product peaks are close to, but do not agree exactly with those of an authentic sample of $(CH_3)_2C{=}O$ loaded into FAPO-5, presumably because of overlap with decreasing 2-propanol bands. Indeed, a computer-calculated infrared difference spectrum (acetone in FAPO-5 minus 2-propanol in FAPO-5) agrees completely with the photolysis difference spectrum of Figure 1b. Only the product absorptions at 1625 and 3400 cm^{-1} do not appear in the simulated spectrum. Band positions and ^{18}O shifts confirm their assignment to the bending and stretching absorption, respectively, of H_2O coproduct. We conclude that excitation of FAPO-5 at 355 nm induces oxidation of 2-propanol to acetone.

$$(CH_3)_2CH{-}OH + O_2 \xrightarrow[\text{FAPO-5}]{355\ \text{nm}} (CH_3)_2CH{=}O + H_2O$$

The reaction rate was found to be linear in laser photolysis power, indicating a single photon photochemical process. In a typical experiment using 145 mW cm^{-2} photolysis power, 18% of the 2-propanol loaded into the sieve was converted to acetone in 1 h. The quantum efficiency to reaction was calculated as the product growth per photon absorbed. On the basis of the measured extinction coefficient of the acetone 1711 cm^{-1} ν(C═O) band in FAPO-5, the growth of this absorption upon photolysis, the photolysis photon flux, and the fraction of light absorbed at 355 nm, we calculate a quantum yield of 0.1, when using 250 Torr of O_2.

In addition to photolysis at 355 nm, irradiation was also conducted at 389 and 423 nm. As can be seen from Figure 2, the relative yields at these longer wavelengths follow fairly closely the absorption profile of the charge-transfer band. Note that none of these photolysis wavelengths coincides with an absorption of the alcohol or O_2 molecule. The deviation of the reaction yield from the absorption profile around 420 nm does not signal a lower quantum efficiency since we observed that the peak of the Fe(III) d−d transition[18] essentially vanishes upon adsorption of the reactants onto the sieve.

As shown in Figure 3, two C═O stretch absorptions grow in upon photooxidation of 2-propanol by $^{18}O_2$. One originates from $(CH_3)_2C{=}^{16}O$ absorbing at 1711 cm^{-1}, the other from

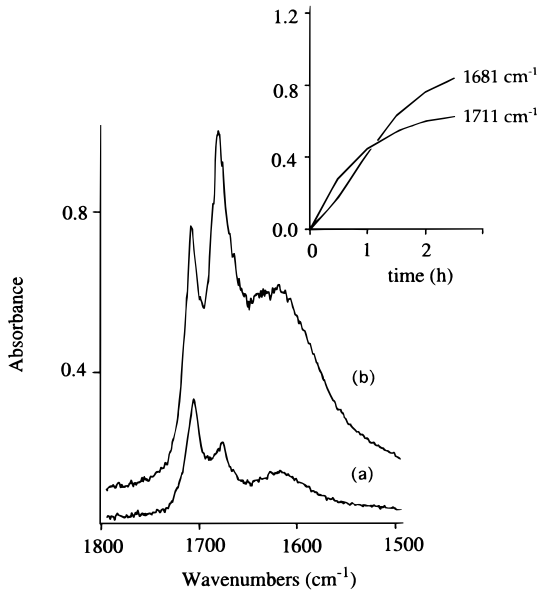

Figure 3. Infrared difference spectra upon photoinduced 2-propanol + $^{18}O_2$ reaction in FAPO-5 at 21 °C: (a) 30 min irradiation at 355 nm, 145 mW cm^{-2}; (b) 150 min photolysis under same conditions. Insert: kinetics of peak absorbance growth at 1681 and 1711 cm^{-1}.

$(CH_3)_2C{=}^{18}O$ absorbing at 1681 cm^{-1}. Spectra and kinetic curves (insert) of Figure 3 show that the ^{18}O-labeled acetone exhibits an induction period while the parent product does not. This indicates that unlabeled acetone is the primary oxidation product, with the oxygen atom originating from the alcohol. Subsequent photochemical $^{16}O{-}^{18}O$ exchange of acetone under UV light in the presence of $^{18}O_2$ explains the growth behavior of $(CH_3)_2C{=}^{18}O$, as this was established by a separate experiment in which an authentic sample of acetone was loaded into FAPO-5 together with $^{18}O_2$ gas and irradiated at 355 nm. Under similar photolysis conditions as used in the 2-propanol photolysis experiment, approximately half of the $(CH_3)_2C{=}O$ was converted to $(CH_3)_2C{=}^{18}O$ within 2 h. In the absence of light, no exchange took place.

2. Photooxidation of Methanol by O_2. Methanol gas (typically 6 Torr) exposed to a dehydrated FAPO-5 pellet at room temperature resulted in infrared peaks of the adsorbed CH_3OH at 1347 (shoulder), 1436, 1472, 2843, 2956, 3250, and 3619 cm^{-1}. As in the case of 2-propanol discussed above, methanol adsorbed on FAPO-5 has a free OH stretch (3619 cm^{-1}) as well as a very broad, H-bonded OH absorption (3250 cm^{-1}). The region 1900−1300 cm^{-1} of the spectrum is shown in Figure 4a. Loading of 250 Torr of O_2 did not result in any reaction at room temperature even over periods of tens of hours. On the other hand, excitation of the FAPO-5 charge-transfer band with 355 nm light led to depletion of methanol under concurrent growth at 1385, 1436 (very weak), 1456 (very weak), 1622, 1675 (shoulder), 1717, and 3500 cm^{-1} (broad). The last-mentioned band overlaps strongly with the very broad, decreasing OH stretch of methanol. Conducting the photolysis experiment under identical conditions with $^{18}O_2$ gave product growth at 1385, 1436, 1456, 1616, 1684, 1717, and around 3500 cm^{-1} (broad). Photolysis difference spectra of the CH_3OH + $^{16}O_2$ and CH_3OH + $^{18}O_2$ reactions are presented as traces b and c, respectively, of Figure 4. Product spectra just described did not change when irradiating at longer photolysis wavelengths. Similar to the 2-propanol case, the relative yields were proportional to the number of photons absorbed by the FAPO-5 charge-transfer tail at three different wavelengths, namely, 355, 389, and 423 nm, as can be seen from Figure 2. This indicates

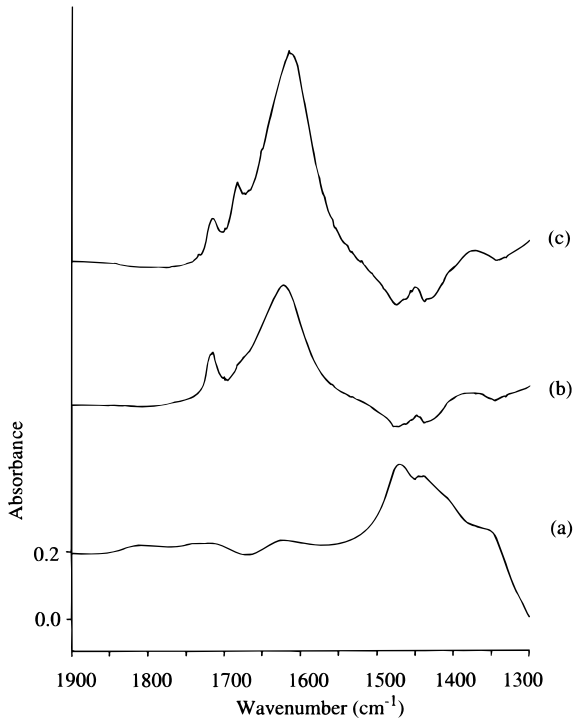

Figure 4. 355 nm induced $CH_3OH + O_2$ reaction in FAPO-5 at room temperature. (a) Infrared difference spectrum upon loading of 6 Torr methanol and 250 Torr of O_2 into FAPO-5. (b) Difference of spectra before and after 240 min irradation of the CH_3OH and $^{16}O_2$ loaded sieve at 355 nm. (c) Difference spectra following 230 min photolysis of CH_3OH (5 Torr) and $^{18}O_2$ (230 Torr) loaded sieve.

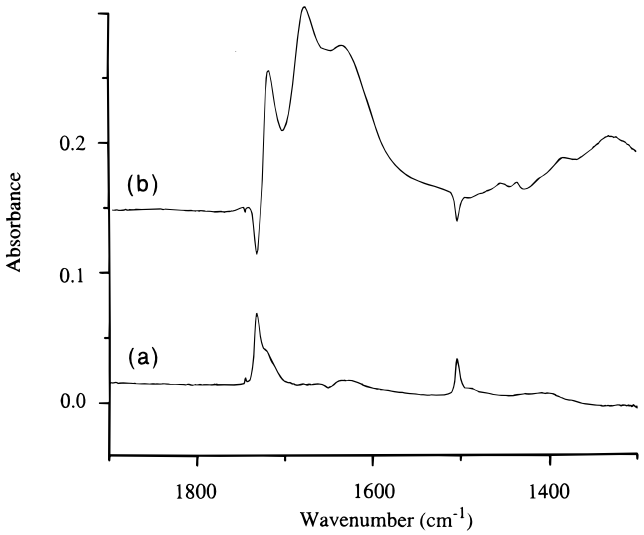

Figure 5. Spontaneous dark reaction of formaldehyde loaded into FAPO-5. (a) Infrared spectrum immediately after loading of 1 Torr of $CH_2{=}O$. (b) Difference spectrum after 19 h in the dark.

that the quantum efficiency remains constant, within uncertainties, across the charge-transfer absorption profile.

The position of the broad, intense product band at 1622 cm^{-1} and its ^{18}O shift of 6 cm^{-1} are characteristic for the bending mode of H_2O.[26] The extremely broad OH stretch feature around 3500 cm^{-1} confirms that water is a reaction product. The 1717 cm^{-1} absorption has a 33 cm^{-1} ^{18}O shift, indicative of a product with a C═O group. However, the band does not coincide with the C═O stretch of formaldehyde, the likely product of CH_3OH oxidation by analogy to the 2-propanol + O_2 reaction. As can be seen from Figure 5, trace a, $CH_2{=}O$ gas loaded into FAPO-5 sieve has intense absorptions at 1732 and 1504 cm^{-1}. Neither of these bands is observed in the $CH_3OH + O_2$ photoproduct spectrum. On the other hand, the 1717 cm^{-1} band and the very weak but sharp peaks at 1456 and 1436 cm^{-1} coincide with those of an authentic sample of HCO_2CH_3 in FAPO-5, indicating that methyl formate is a reaction product. The bands agree well with ν(C═O) and the two CH_3 bending modes of the stable cis conformer of isolated HCO_2CH_3.[27] The fact that the C═O stretch splits into bands at 1717 and 1684 cm^{-1} signals that both isotopomers $HC(=O)OCH_3$ and $HC(=^{18}O)OCH_3$ are generated upon photoreaction of methanol with $^{18}O_2$.

Formation of the HCO_2H is signaled by the broad product band at 1385 cm^{-1} and a shoulder at 1675 cm^{-1} both of which coincide with absorptions of formic acid loaded into FAPO-5 or iron-free $AlPO_4$ sieve from the gas phase. HCO_2H in FAPO-5 shows, in addition, a broad band at 1625 cm^{-1}, which lies close to the intense asymmetric CO_2 stretch of HCO_2^- observed at 1611 cm^{-1} when impregnating sodium formate into FAPO-5. This band agrees with the literature IR spectrum of the salt.[28] Hence, HCO_2^- or HCO_2 interacting with an Fe center may contribute intensity to the broad absorption of H_2O product at 1620 cm^{-1}. In the absence of more details on the nature of the formate species, we designate the 1620 cm^{-1} product simply as formate. No other photoproduct was formed. Specifically, no CO_2 was found, readily detectable by its intense absorption at 2360 cm^{-1}.

Formaldehyde loaded into FAPO-5 sieve was found to undergo a slow, spontaneous reaction in the dark at room temperature. After 1 h, the $CH_2{=}O$ peaks at 2989, 2898, 2825, 1732, and 1504 cm^{-1} (which agree well with literature IR data)[29,30] have decreased by about two-thirds under concurrent product growth at 1717, 1675, 1633, 1456, 1436, and 1385 cm^{-1}. These bands are readily assigned to HCO_2CH_3 (1717, 1456, 1436), HCO_2H (1675, 1385), and formate (1633) as they coincide with the $CH_3OH + O_2$ photoproduct absorptions discussed above. An infrared difference spectrum taken after 19 h is shown in Figure 5b. The difference spectra at early times show a bleach at 1640 cm^{-1}, which is due to loss of residual H_2O upon reaction of $CH_2{=}O$ (the absorption of residual H_2O following dehydration of the sieve at 200 °C is typically 0.2 absorbance units). This suggests that formaldehyde is depleted by the Cannizzaro reaction,

$$2CH_2{=}O + H_2O \rightarrow HCO_2H + CH_3OH \rightarrow HCO_2CH_3 + H_2O$$

followed by condensation of some fraction of the formic acid and methanol so produced to methyl formate.[31,32] Since Cannizzaro reactions in solution are base-catalyzed, it suggests that the solvent-free sieve has basic character. Strong support for this mechanism of the spontaneous transformation of formaldehyde stems from the observations that FAPO-5 sieve pretreated by $H_2{}^{18}O$ (three cycles of dehydration of the sieve followed by exposure to $H_2{}^{18}O$ gas) and loaded with $CH_2{=}O$ yields $HC^{18}OOCH_3$. While the formation of HCO_2H indicates that Cannizzaro reaction is the prevailing mechanism, we cannot rule out that some methyl formate product originates from direct reaction of two formaldehyde molecules by the Tishchenko mechanism.[32] Note that involvement of Fe centers in the dark reaction of formaldehyde is ruled out by two observations. First, UV−vis diffuse reflectance spectroscopy did not indicate any decrease of the Fe^{+III} concentration, which would occur if $CH_2{=}O$ reduces the Fe centers. Second, the same spontaneous reaction of formaldehyde was observed in a molecular sieve free of Fe (TS-1).[33]

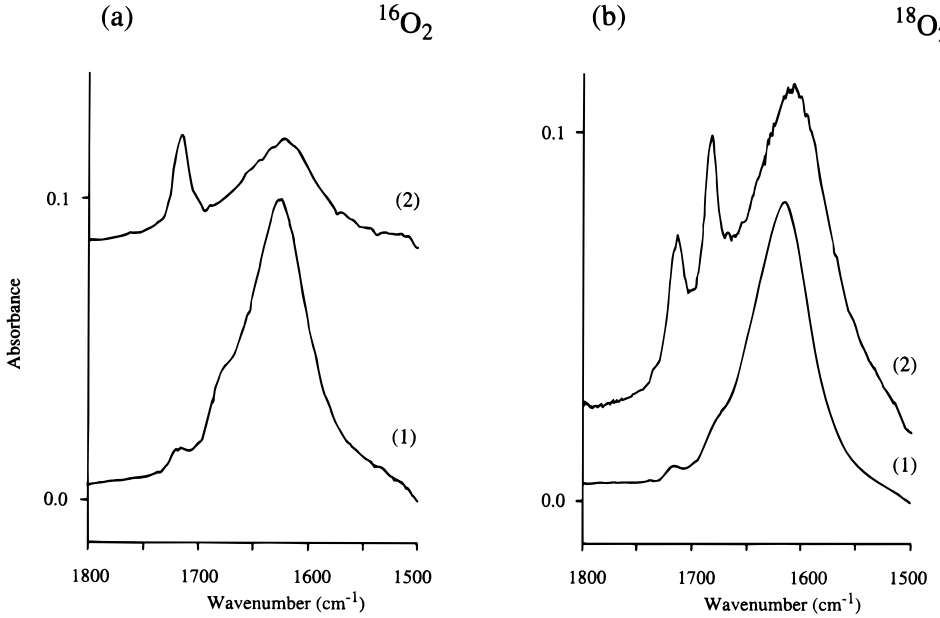

Figure 6. Kinetics of formic acid and H_2O product growth in FAPO-5. Infrared difference spectra upon $CH_3OH + {}^{16}O_2$ photolysis. (b) Difference spectra following $CH_3OH + {}^{18}O_2$ photolysis. Trace 1 represents the difference spectrum after 30 min irradiation; trace 2 shows the difference between 240 and 180 min photolysis.

Loading of $CD_2{=}O$ into FAPO-5 sieve furnished additional support for the product assignment. The 1717 cm^{-1} ν(C═O) product peak observed in the case of $CH_2{=}O$ exhibits a red shift of 30 cm^{-1} as expected for DC(═O)OCD$_3$.[27] On the other hand, the 1675 cm^{-1} absorption of the $CH_2{=}O$ conversion product shows only a 15 cm^{-1} red shift in the $CD_2{=}O$ product spectrum, indicating that it originates from DCO_2H[34] (this mode involves a Fermi resonance between ν(C═O) and the overtone of δ(C═D)).[35] This is the expected isotopomer of the Cannizzaro reaction of $CD_2{=}O$ with H_2O and corroborates our assignment of the 1675 cm^{-1} peak. The product bands of the thermal conversion of $CD_2{=}O$ agree with the photochemical products of the $CD_3OD + O_2$ reaction in FAPO-5. In the latter experiment, the intense 1622 cm^{-1} absorption of the $CH_3OH + O_2$ product spectrum is replaced by a much weaker band of 1613 cm^{-1}. This is consistent with the fact that no H_2O is produced and that the asymmetric CO_2 stretch of HCO_2^-, contributing to the 1622 cm^{-1} absorption, undergoes the expected 10 cm^{-1} red shift of DCO_2^-.[36]

Spectroscopy of thermal $CH_2{=}O$ and $CD_2{=}O$ reactions in FAPO-5 sieve suggests that the observed products HCO_2H, formate, and HCO_2CH_3 of the LMCT-induced $CH_3OH + O_2$ photoreaction are secondary thermal products of initially generated $CH_2{=}O$. Since H_2O is a stoichiometric reaction product, the Cannizzaro reaction is fast and no build-up of $CH_2{=}O$ is expected. Note that the formation of $HC^{18}OOCH_3$ in the case of the $CH_3OH + {}^{18}O_2$ system is consistent with the fact that one O of the final product originates from the alcohol, the other from H_2O. Water is the final product of O_2 reduction and presumably emerges from disproportionation of initially formed H_2O_2 due to the catalytic effect of the Fe centers[37] and the basic character of the sieve[38]

$$H_2O_2 \rightarrow H_2O + \frac{1}{2}O_2$$

The growth of methyl formate exhibits a pronounced induction period, as can be seen from Figure 6. The absorbance increase of the 1717 cm^{-1} HCO_2CH_3 band is delayed relative to the H_2O product at 1620 cm^{-1} (Figure 6a), as is the growth of the ester bands at 1717 and 1684 cm^{-1} in the $CH_3OH + {}^{18}O_2$ case (Figure 6b). Clearly, ester formation is a secondary thermal process. We infer from these observations that FAPO-5-mediated $CH_3OH + O_2$ photoreaction yields $CH_2{=}O$ and H_2O_2 as primary redox products.

SCHEME 1

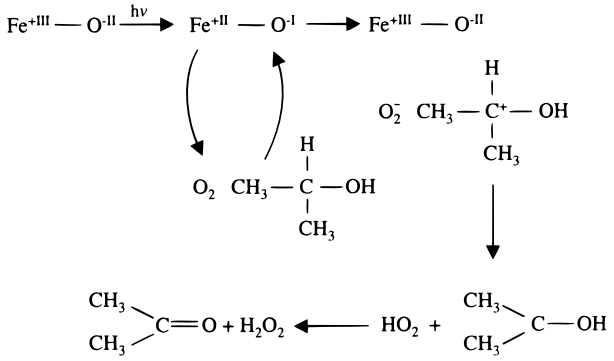

IV. Discussion

The UV−vis absorption tail of FAPO-5 molecular sieve is assigned to a ligand-to-metal charge-transfer transition approximately described by $Fe^{+III}{-}O^{-II} \rightarrow Fe^{+II}{-}O^{-I}$.[18] This assignment is further supported by the recent observation of this transition in a related Fe framework substituted silicoaluminophosphate sieve (FAPSO-37).[39] Scheme 1 illustrates our proposed mechanism of how this excited state initiates reaction in the case of the 2-propanol + O_2 system. The initial event following excitation of the charge-transfer state is most probably electron transfer from the reduced Fe to O_2, resulting in the formation of O_2^- under concurrent oxidation of the alcohol by the hole centered on the O ligand. Organic radical cations are known to be extremely acidic ($pK_a \leq -10$).[40] Hence, proton transfer to O_2^- is expected to yield HOO and hydroxypropyl radical $(CH_3)_2{-}COH$ on a fast (presumably nanosecond or shorter) time scale. The rather high quantum yield of reaction indicates that this proton-transfer quenching of the alcohol radical cation/superoxide pair competes successfully with back

electron transfer. H^+-transfer may involve deprotonation of O rather than C, resulting in the initial formation of alkoxy radical $(CH_3)_2CH-O$. However, rapid rearrangement to the more stable $(CH_3)_2C-OH$ radical may occur.[41] The final product most likely emerges from direct abstraction of H from the hydroxypropyl radical by HOO. It is also conceivable that the two radicals first combine to form $(CH_3)_2C(O_2H)OH$, followed by elimination of H_2O_2. In fact, the latter has been proposed as an intermediate of thermal 2-propanol oxidation.[37] However, direct H abstraction is more likely because we were unable to trap any intermediate when conducting 2-propanol photooxidation at −90 °C. A closed-shell molecule such as $(CH_3)_2C(O_2H)OH$ is expected to be stabilized at such a low temperature. In any case, the proposed mechanism is consistent with the single photon nature of the photochemistry and the fact that the primary products of the photoreaction of 2-propanol-^{16}O with $^{18}O_2$ are acetone-^{16}O and $H_2{}^{18}O$.

Enthalpies of formation of $(CH_3)_2CH-OH$ (−65.2 kcal mol^{-1}),[42] HOO radical (5.0 kcal mol^{-1}),[43] and $(CH_3)_2CHO$ radical (−12.5 kcal mol^{-1})[44] give an endothermicity of 58 kcal mol^{-1} for the conversion of 2-propanol and O_2 to the radical pair. Hence, the observation that the reaction can be initiated with photons as low in energy as 420 nm (68 kcal mol^{-1}) is consistent with the proposed mechanism.

The proposed mechanism for CH_3OH photooxidation by O_2 is analogous to that of 2-propanol, leading to a CH_2OH/HOO radical pair. Hydroxymethyl radical is an established species.[30] On the basis of enthalpies of formation ($\Delta H_f^\circ(CH_3OH) = -48$ kcal mol^{-1}; $\Delta H_f^\circ(HOO) = 5.0$ kcal mol^{-1}; $\Delta H_f^\circ(CH_3O^\bullet) = 4.2$ kcal mol^{-1}),[41,43] we estimate an endothermicity of 57 kcal mol^{-1} for the reaction step

$$CH_3OH + O_2 \xrightarrow{h\nu} CH_3OH^+ + O_2^- \rightarrow CH_3O^\bullet + HOO$$

which, most probably, is followed by isomerization to CH_2OH before H abstraction leads to $CH_2{=}O$ and H_2O_2.[45] The finding that loading of $CH_2{=}O$ into the molecular sieve results in spontaneous Cannizzaro reaction explains why HCO_2H, formate, and HCO_2CH_3 are the observed final oxidation products, rather than formaldehyde.

The rather efficient photoreaction of O_2 and alcohol at the gas−micropore interface of FAPO-5 implies that the transient Fe^{+II} centers of the molecular sieve reduce O_2 in a thermoneutral or exoergic step

$$Fe^{+II}(FAPO\text{-}5) + O_2 \rightarrow Fe^{+III}(FAPO\text{-}5) + O_2^- \quad \Delta\epsilon^\circ > 0$$

The standard potential for one-electron reduction of O_2 is known to vary only modestly between aqueous solution (−0.33 V vs NHE) and aprotic media (−0.55 V vs NHE) and is independent of electrode material or pH.[38] Therefore, O_2 is a useful probe for redox properties of framework metal centers. The efficient photoreduction in FAPO-5 implies that the reduction potential of transient Fe^{+II} centers is at least as negative. This is more than 0.6 V more negative than the reduction potential of conduction band electrons of dense-phase Fe_2O_3 semiconductor particles (0.3 V).[46] It suggests that the photoreduced framework Fe centers of the molecular sieve are substantially more strongly reducing than the Fe_2O_3 conduction band electrons. This may reflect the less stable tetrahedral coordination into which Fe centers are forced by the aluminophosphate framework. Iron in the +2 oxidation state prefers octahedral coordination.[47] Loss of stability of Fe^{+II} is expected to increase the reducing strength of the metal center. This shift toward more negative reduction potential of LMCT-excited FAPO-5 sieve compared to band-gap excited iron oxide materials is particularly interesting to photoactivation of molecules that are difficult to reduce, such as carbon oxides.

V. Conclusions

In situ monitoring of probe reactions by FT-IR spectroscopy has been employed to explore the reactivity of LMCT-excited framework Fe centers of FAPO-5 at the gas−micropore interface. According to the mechanism inferred from the observed products, O_2 acts as one-electron acceptor, thereby reoxidizing the photoreduced Fe^{+II}. Concurrently, methanol or 2-propanol molecules act as donors and reduce the transient hole on framework oxygen. Subsequent proton transfer and H atom abstraction leads to formaldehyde (acetone) and H_2O_2, resulting in an overall two-electron transfer process. Among these products, acetone is stable in the sieve, while formaldehyde undergoes fast Cannizzaro reaction and H_2O_2 disproportionates to H_2O and O_2. The finding that O_2 is reduced efficiently by transient framework Fe^{+II} suggests that its reduction potential lies at least one-half of a volt more negative than that of the conduction band of dense-phase Fe_2O_3 particles. This may open up demanding photoreductions not accessible by photochemistry at iron oxide semiconductor materials. Using this method of in situ FT-IR monitoring of laser-induced chemistry, we will explore reactions with probe molecules covering a range of electron acceptor and donor strengths that will allow us to bracket the redox potentials of excited framework metals at the gas−micropore interface. This will furnish the basis needed for selecting microporous materials with appropriate framework metals and oxidation states for a desired photochemical transformation.

Acknowledgment. This work was supported by the Director, Office of Science, Office of Basic Energy Sciences, Chemical Sciences Division of the U.S. Department of Energy under Contract DE-AC03-76SF00098.

References and Notes

(1) Balzani, V.; Carassiti, V. *Photochemistry of Coordination Compounds*; Academic Press: New York, 1970.

(2) Blatter, F.; Sun, H.; Vasenkov, S.; Frei, H. *Catal. Today* **1998**, *41*, 297 and references therein.

(3) (a) Vasenkov, S.; Frei, H. *J. Am. Chem. Soc*. **1998**, *120*, 4031. (b) Vasenkov, S.; Frei, H. Submitted.

(4) Anpo, M.; Zhang, S. G.; Yamashita, H. In *Studies in Surface Science and Catalysis*; Hightower, J. W., Delgass, W. N., Iglesia, E., Bell, A. T., Eds.; Elsevier: Amsterdam, 1996; Vol. 101, p 941.

(5) Zhang, S. G.; Ichihashi, Y.; Yamashita, H.; Tatsumi, T.; Anpo, M. *Chem. Lett.* **1996**, 895.

(6) Anpo, M.; Zhang, S. G.; Mishima, H.; Matsuoka, M.; Yamashita, H. *Catal. Today* **1997**, *39*, 159.

(7) Zhang, S. G.; Fujii, Y.; Yamashita, H.; Koyano, K.; Tatsumi, T.; Anpo, M. *Chem. Lett*. **1997**, 659.

(8) Higashimoto, S.; Zhang, S. G.; Yamashita, H.; Matsumura, Y.; Somua, Y.; Anpo, M. *Chem. Lett.* **1997**, 1127.

(9) Zhang, S. G.; Ariyukai, M.; Mishima, H.; Higashimoto, S.; Yamashita, H.; Anpo, M. *Microporous Mesoporous Mater*. **1998**, *21*, 621.

(10) Anpo, M.; Yamashita, H.; Ikeue, K.; Fujii, Y.; Zhang, S. G.; Ichihashi, Y.; Park, D. R.; Suzuki, Y.; Koyano, K.; Tatsumi, T. *Catal. Today* **1998**, *44*, 327.

(11) Meier, W. M.; Olson, D. H.; Baerlocher, Ch. *Atlas of Zeolite Structure Types*, 4th ed.; Elsevier: London, 1996; p 26.

(12) *Introduction to Zeolite Science and Practice*; van Bekkum, H., Flanigen, E. M., Jansen, J. C., Eds.; Studies in Surface Science and Catalysis, Vol. 58; Elsevier: Amsterdam, 1991.

(13) Li, H. X.; Martens, J. A.; Jacobs, P. A.; Schubert, S.; Schmidt, F.; Ziethen, H. M.; Trautwein, A. X. In *Studies in Surface Science and Catalysis*; Grobet, P. J., Mortier, W. J., Vansant, E. F., Schulz-Ekloff, G., Eds.; Elsevier: Amsterdam, 1988; Vol. 37, p 75.

(14) Schubert, S.; Ziethen, H. M.; Trautwein, A. X.; Schmidt, F.; Li, H. X.; Martens, J. A.; Jacobs, P. A. In *Studies in Surface Science and*

Catalysis; Karge, H. G., Weitkamp, J., Eds.; Elsevier: Amsterdam, 1989; Vol. 46, p 735.

(15) Ojo, A. F.; Dwyer, J.; Parish, R. V. In *Studies in Surface Science and Catalyis*; Jacobs, P. A., van Santen, R. A., Eds.; Elsevier: Amsterdam, 1989; Vol. 49, p 227.

(16) Cardile, C. M.; Tapp, N. J.; Milestone, N. B. *Zeolites* **1990**, *10*, 90.

(17) Pang, W.; Qiu, S.; Kan, Q.; Wu, Z.; Peng, S.; Fan, G.; Tian, D. In *Studies in Surface Science and Catalysis*; Jacobs, P. A., van Santen, R. A., Eds.; Elsevier: Amsterdam, 1989; Vol. 49, p 281.

(18) Park, J. W.; Chon, H. *J. Catal*. **1992**, *133*, 159.

(19) Hartmann, M.; Kevan, L. *Chem. Rev*. **1999**, *99*, 635.

(20) (a) Wilson, S. T.; Lok, B. M.; Flanigen, E. M. U.S. Patent 4,310,440, 1982. (b) Wilson, S. T.; Lok, B. M.; Messina, C. A.; Cannan, T. R.; Flanigen, E. M. *J. Am. Chem. Soc.* **1982**, *104*, 1146.

(21) Treacy, M. M. J.; Higgins, J. B.; von Ballmoos, R. *Zeolites* **1996**, *16*, 352.

(22) Lasocha, W.; Lewinski, K. *PROSZKI Program*, version 2.4; Jagiellonian University: Krowkow, Poland.

(23) Jeong, M. S.; Frei, H. *J. Mol. Catal. A: Chemical*, in press.

(24) Blatter, F.; Frei, H. *J. Am. Chem. Soc*. **1994**, *116*, 1812.

(25) Spence, R.; Wild, W. *J. Chem. Soc. (London)* **1935**, 338.

(26) Tso, T. L.; Lee, E. K. C. *J. Phys. Chem*. **1985**, *89*, 1612.

(27) Müller, R. P.; Hollenstein, H.; Huber, R. J. *J. Mol. Spectrosc*. **1983**, *100*, 95.

(28) Colthup, N. B.; Daly, L. H.; Wiberley, S. E. *Introduction to Infrared and Raman Spectroscopy*, 3rd ed.; Academic Press: New York, 1990; p 317.

(29) Herzberg, G. *Infrared and Raman Spectra*; Van Nostrand: New York, 1945; p 300.

(30) Jacox, M. E. *Chem. Phys*. **1981**, *59*, 213.

(31) Roberts, J. D.; Caserio, M. C. *Basic Principles of Organic Chemistry*; Benjamin: New York, 1964; p 461.

(32) March, J. *Advanced Organic Chemistry*, 4th ed.; Wiley: New York, 1992; p 1233.

(33) Ulagappan, N.; Frei, H. In preparation.

(34) Millikan, R. C.; Pitzer, K. S. *J. Chem. Phys*. **1957**, *27*, 1305.

(35) Redington, R. L. *J. Mol. Spectrosc.* **1977**, *65*, 171.

(36) Greenler, R. G. *J. Chem. Phys*. **1962**, *37*, 2094.

(37) Cotton, F. A.; Wilkinson, G. *Advanced Inorganic Chemistry*, 5th ed.; Wiley: New York, 1988; p 456.

(38) Wilshire, J.; Sawyer, D. T. *Acc. Chem. Res*. **1979**, *12*, 105.

(39) Spinace, E. V.; Cardoso, D.; Schuchardt, U. *Zeolites* **1997**, *19*, 6.

(40) Hammerich, O.; Parker, V. D. *Adv. Phys. Org. Chem*. **1984**, *20*, 55.

(41) Hucknall, D. J. *Chemistry of Hydrocarbon Combustion*; Chapman and Hall: London, 1985; p 302.

(42) Pedley, J. B.; Naylor, R. D.; Kirby, S. P. *Thermochemical Data of Organic Compounds*, 2nd ed.; Chapman and Hall: London, 1986; p 116.

(43) Benson, S. W. *Thermochemical Kinetics*; Wiley: New York, 1968.

(44) Hucknall, D. J. *Chemistry of Hydrocarbon Combustion*; Chapman and Hall: London, 1985; p 296.

(45) (a) Radford, H. E. *Chem. Phys. Lett*. **1980**, *71*, 195. (b) Radford, H. E.; Evenson, K. M.; Jennings, D. A. *Chem. Phys. Lett*. **1981**, *78*, 589.

(46) Kamat, P. V. *Chem. Rev*. **1993**, *93*, 267.

(47) Cotton, F. A.; Wilkinson, G. *Advanced Inorganic Chemistry*, 5th ed.; Wiley: New York, 1988; p 711.